Studies on Axial Effective Thermal Conductivities in Packed Beds

SAKAE YAGI, DAIZO KUNII, and NORIAKI WAKAO

University of Tokyo, Tokyo, Japan

The axial effective thermal conductivities of packed beds were determined by measuring the axial temperature gradients at steady state, the heat being conducted in the direction opposite to that of air. The present experiments were carried out with the beds of glass beads, metallic balls, broken pieces of limestone, and Raschig rings, taken in separate experiments.

It was found that the axial effective thermal conductivity increases more with the increase of air flow than it does in the case of radial conductivity. The axial effective thermal conductivity coincides with the radial conductivity when $N_{Re} \to 0$.

In process design of nonisothermal packed-bed reactors knowledge of the effective thermal conductivity is required, as well as that of the effective mass diffusivity. While there have been numerous investigations on the radial effective thermal conductivity (*14* through *17*, *22*) and the radial effective mass diffusivity (*2*, *7*, *14*), less attention has been paid to the effective thermal conductivity in the axial direction. On the other hand intense attention has been focused recently on the mixing of fluid in the axial direction through the packed beds, and consequently many experimental investigations (*3* to *6*, *10*, *12*, *18*) and mathematical treatments (*1*, *8*, *11*, *21*) have been presented.

As pointed out experimentally (*9*, *13*) and mathematically (*20*) it is not always justifiable to neglect the thermal conduction in the axial direction in calculating the axial temperature gradients of packed-bed reactors. However there has been no effort to study the determination of the effective thermal conductivity in the axial direction.

The authors have carried out the axial heat transfer experiments of packed beds, where heat from infrared radiation flowed countercurrently to the flow of fluid. By measuring the steady state axial temperature gradients the axial effective thermal conductivities are obtained.

EXPERIMENTAL

Apparatus

In order to carry out the axial heat transfer experiments the adiabatic reactors are used as the containers of packed bed, which are made of the double walled glass tube, the annular space being evacuated and the internal surfaces plated with silver for thermal insulation in the radial direction. Radiation heat supply is maintained at the bed outlet face by means of a strong infrared lamp, and air at room temperature is flowed upwards through the bed. The directions of flow of fluid and heat are opposite to one another.

Reactors of two different sizes are used: 68-mm. I. D., as shown in Figure 1, and 50-mm. I. D.; these are identical to one another except for the sizes. The copper-constantan thermocouples are installed axially from about 1 cm. down the bed outlet in the center as well as near the wall in the same level.

Procedure

After the infrared lamp is switched on, it takes from 60 to 100 min. to attain the steady state, and then the temperatures and the flow rate are recorded. The solid particles used for these experiments are glass beads, metallic balls, broken pieces of limestone, and Raschig rings, details of which are listed in Table 1.

THEORETICAL TREATMENT

In ordinary process design method for packed-bed reactors the temperature difference between solid and fluid is usually neglected, and the concept of the effective thermal conductivities in axial as well as radial direction is then considered.

Therefore in this section it is assumed that the temperatures of solid and fluid are approximately the same. The apparatus used in the experiments is shown in Figure 1. The heat balance for the differential height dl may be represented as

$$C_p G \frac{dt}{dl} + k_{e,z} \frac{d^2t}{dl^2} = 0 \qquad (1)$$

The above equation involves the assumptions that $k_{e,z}$ and C_pG are constant in the bed, as far as the mean values are concerned. The solution of Equation (1) is therefore

$$\frac{t - t_i}{t_o - t_i} = e^{-\frac{C_p G}{k_{e,z}} l} \qquad (2)$$

EXPERIMENTAL RESULTS

The calculation of the axial effective thermal conductivity is made as follows: The difference of the temperature measured in the axial direction and of the inlet air; that is $t - t_i$, is plotted against bed depth l in a semilogarithmic graph. A graph for a typical run is shown in Figure 2. Equation (2) may thus be rewritten as

TABLE 1. SOLIDS USED FOR EXPERIMENTS

Solid	Nominal diameter, mm.	D_p, mm.	Void fraction, ϵ	Thermal conductivity of solid, kcal./(m.)(hr.)(°C.)
Glass beads	0.99 ~ 0.83	0.91	0.40*	0.50
	2.6	2.6		
	6.0	6.0		
Steel balls	3.0	3.0	0.40*	40
	4.8	4.8		
Lead shots	1.5	1.5	0.40	30
Limestone broken pieces	1.4 ~ 1.2	1.3	0.43*	1.2
	2.4 ~ 1.7	2.0		
	3.9 ~ 3.0	3.4		
Porcelain Raschig rings	4 × 4 thickness 1.0	4.0	0.50	1.4
	9 × 9 thickness 1.3	9.0	0.69	

* Mean values.

TABLE 2. TYPICAL DATA OF AXIAL EFFECTIVE THERMAL CONDUCTIVITIES

Run-no.	Air mass velocity G, kg./m.^{2} hr.	Inlet air temp., t_i, °C.	Temp.† at T_1, °C.	Temp.* gradient, cm.$^{-1}$	Reynolds number N_{Re}	$k_{e,z}/k_g$
Limestone, D_P = 1.3 mm., bed diam. D_T = 68 mm.						
(C) — 45	217	14	120	0.770	3.85	11.7
46	176	15	140	0.666	3.05	10.7
47	181	15	130	0.690	3.17	10.7
48	142	15	120	0.555	2.51	10.6
49	114	15	130	0.444	2.00	10.5
Limestone, D_P = 2.0 mm., bed diam. D_T = 68 mm.						
(C) — 50	262	16	140	0.740	6.99	14.3
51	284	16	130	0.770	7.65	15.0
52	439	10	90	1.11	12.4	17.0
53	309	12	100	0.833	8.65	15.8
54	269	13	120	0.770	7.34	14.4
55	197	15	120	0.625	5.37	13.0
56	159	16	130	0.488	4.29	13.3
Limestone, D_P = 3.4 mm., bed diam. D_T = 68 mm.						
(C) — 58	276	18	110	0.667	12.9	17.2
59	214	18	130	0.589	9.78	14.8
60	184	17	120	0.500	8.50	15.2
61	135	17	120	0.408	6.24	13.6
62	66.6	17	130	0.232	3.05	11.7

* Value of slope $C_pG/k_{e,z}/2.303$ as obtained by plotting values of log $(t-t_i)$ against axial distance l.
† See Figure 1 for T_1.
Physical properties of air are those at mean temperature of bed.

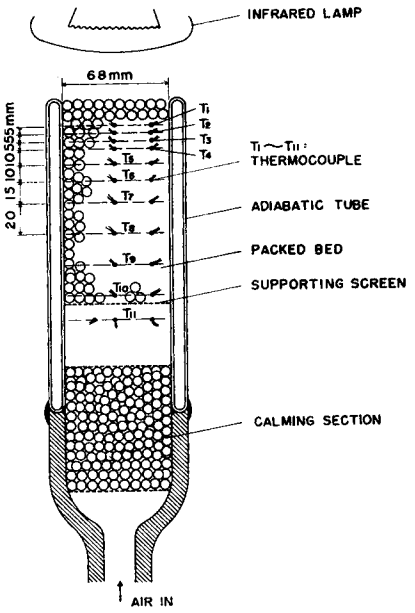

Fig. 1. Experimental apparatus used for axial heat transfer.

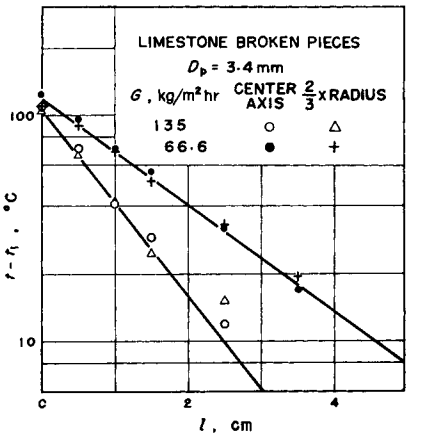

Fig. 2. Examples of experimentally observed axial temperature gradients in beds of broken pieces of limestone.

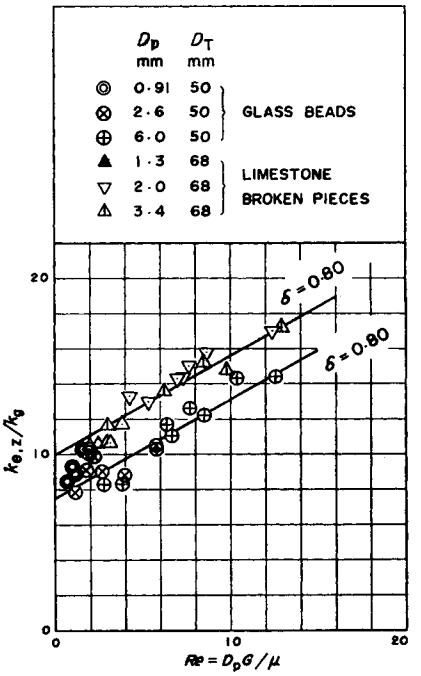

Fig. 3. Data for glass beads and broken pieces of limestone.

$$\ln (t - t_i) = \text{const} - \frac{C_pG}{k_{e,z}} l$$

As is shown in the above equation the slope of the straight line drawn in a semilogarithmic graph should be equal to $-C_pG/k_{e,z}/2.303$. Thus from the slope determined above and the air mass velocity for a given run $k_{e,z}$ is calculated.

It is not always possible to draw the straight line through all the points on a semilogarithmic graph. The straight lines were located by eye only within the regions of comparatively large values of $t - t_i$, since the low values in a semilogarithmic graph may incur experimental errors and are also likely to cause error in locating the lines. It is evident that the accuracy with which the slopes are obtained influences the accuracy of the derived values of $k_{e,z}$. Since the axial temperature gradients become very steep under comparatively high rate of air flow, the present experiments were carried out only for the region of low rate of air flow. The straight lines determined are those drawn free hand with emphasis on the upper portion of the bed where the values of $t - t_i$ are large. In this range the deviations of the values from the straight line are within ± 20% of the derived results of $k_{e,z}$.

The typical data of the experimentally determined axial temperature gradient $C_pG/k_{e,z}/2.303$ and the derived results of $k_{e,z}$ in the dimensionless expression of $k_{e,z}/k_g$ with the experimental conditions are presented in Table 2*. The derived results are shown as $k_{e,z}/k_g$ against $N_{Re} = D_pG/\mu$ in Figures 3 and 4, which show that $k_{e,z}$ is to some extent proportional to N_{Re}. The axial effective thermal conductivity when rate of air flow is zero, that is $k^\circ_{e,z}$, cannot be experimentally determined; therefore the $k_{e,z}/k_g$ — N_{Re} curve is extrapolated at $N_{Re} = 0$ and the intercepted value is found to be $k^\circ_{e,z}/k_g$.

The final correlation may be expressed by the following equation, similar to that of the radial effective thermal conductivity:

$$\frac{k_{e,z}}{k_g} = \frac{k^\circ_{e,z}}{k_g} + \delta N_{Pr} N_{Re} \qquad (3)$$

From Figures 3 and 4 the values of $k^\circ_{e,z}$ and δ are determined and presented in Table 3, which includes the estimated values of radial effective thermal conductivity with motionless fluid $k^\circ_{e,r}$ by the method of Yagi and

* Tabular material has been deposited as document 6384 with the American Documentation Institute, Photoduplication Service, Library of Congress, Washington 25, D. C., and may be obtained for $1.25 for photoprints or $1.25 for 35-mm. microfilm.

Table 3. Experimentally Determined Data of $k^\circ_{e,z}/k_g$ and δ and Calculated Values of $k^\circ_{e,r}/k_g$

Solid	Average diameter D_p, mm.	Experimental range, N_{Re}	Experimental $k^\circ_{e,z}/k_g$*	δ	Calculated† $k^\circ_{e,r}/k_g$
Glass beads	2.6, 6.0	~15	7.5	0.80	7.9, 8.4
Steel balls	4.8	~50	13	0.70	19
Limestone broken pieces	2.0, 3.4	~15	10	0.80	10, 10
Porcelain Raschig rings	4.0, 9.0	~40	7	0.70	9.0, 6.7

* Estimated values, $N_{Re} \to 0$.
† Data used for calculation, (22). Bed mean temp. = 65°C.

	p	ϕ
Glass beads	0.95	0.034
Steel balls	1.0	0.034
Broken pieces	0.50	0.040
Raschig rings	0.50	0.040

Kunii (22). It should be pointed out that the values of $k^\circ_{e,z}$ are almost identical to those of $k^\circ_{e,r}$, and it appears quite natural because the random bed of solids is homogeneous in all directions for heat transfer mechanism in so far as no fluid is flowing.

DISCUSSION

From the present investigations the axial effective thermal conductivities could be correlated to Equation (3). It is interesting to compare the axial effective thermal conductivity with that of the radial direction $k_{e,r}$, which is expressed as (22)

$$\frac{k_{e,r}}{k_g} = \frac{k^\circ_{e,r}}{k_g} + (\alpha\beta) N_{Pr} N_{Re} \quad (4)$$

The value of $(\alpha\beta)$ is of the order of $0.1 \sim 0.3$. Therefore it was found that the extent of the increase of axial effective thermal conductivity with the increase of flow rate was larger than that of radial conductivity.

The present experiments are restricted to a low range of flow rate because the temperature gradient becomes steeper with the increase of the flow rate and it may render the experimental method inadequate. However in many cases it may be in the low flow-rate range that the axial thermal conduction cannot be neglected in the rational design calculations of packed-bed reactors and particularly in controlling the temperature within narrow limits, because the axial temperature gradients are frequently steep under conditions mentioned above.

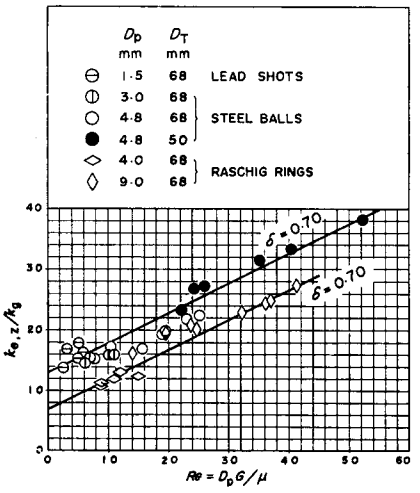

Fig. 4. Data for metallic balls and Raschig rings.

NOTATION

C_p = heat capacity of fluid, kcal./(kg.)(°C.)
D_P = nominal or average diameter of solid, m.
D_T = diameter of packed bed, m.
G = superficial mass velocity of fluid, based on empty column, kg./(sq.m.)(hr.)
$k^\circ_{e,r}$ = radial effective thermal conductivity with motionless fluid, kcal./(m.)(hr.)(°C.)
$k_{e,z}$ = axial effective thermal conductivity, kcal./(m.)(hr.)(°C.)
$k^\circ_{e,z}$ = axial effective thermal conductivity with motionless fluid, kcal./(m.)(hr.)(°C.)
k_g = molecular thermal conductivity of fluid, kcal./(m.)(hr.)(°C.)
l = axial distance variable in direction opposite to flow of fluid, m.
N_{Pr} = $C_p\mu/k_g$ = Prandtl number, dimensionless
N_{Re} = $D_p G/\mu$ = modified Reynolds number, dimensionless
t = temperature of bed, °C.
t_i = temperature of inlet fluid, °C.
t_o = temperature at bed outlet face, °C.
δ = coefficient defined by Equation (3), dimensionless
ϵ = void fraction of bed, dimensionless
μ = viscosity of fluid, kg./(m.)(hr.)
ρ = density of fluid, kg./cu.m.

LITERATURE CITED

1. Aris, Rutherford, and N. R. Amundson, *A. I. Ch. E. Journal*, **3**, 280 (1957).
2. Bernard, R. A., and R. H. Wilhelm, *Chem. Eng. Progr.*, **46**, 233 (1950).
3. Carberry, J. J., and R. H. Bretton, *A. I. Ch. E. Journal*, **4**, 367 (1958).
4. Danckwerts, P. V., *Chem. Eng. Sci.*, **2**, 1 (1953).
5. Deisler, P. F., and R. H. Wilhelm, *Ind. Eng. Chem.*, **45**, 1219 (1953).
6. Ebach, E. A., and R. R. White, *A. I. Ch. E. Journal*, **4**, 161 (1958).
7. Fahien, R. W., and J. M. Smith, *ibid.*, **1**, 28 (1955).
8. Klinkenberg, A., and F. Sjenitzer, *Chem. Eng. Sci.*, **5**, 258 (1956).
9. Kodama, Shinjiro, and Kenichi Fukui, *Chem. Eng. (Japan)*, **12**, 72 (1948).
10. Kramers, H., and G. Alberda, *Chem. Eng. Sci.*, **2**, 173 (1953).
11. Levenspiel, Octave, and W. K. Smith, *ibid.*, **6**, 227 (1957).
12. McHenry, K. W., and R. H. Wilhelm, *A. I. Ch. E. Journal*, **3**, 83 (1957).
13. Ogburn, Hugh, Ph.D. dissertation, Princeton Univ., Princeton, N. J. (1954).
14. Plautz, D. A., and H. F. Johnstone, *A. I. Ch. E. Journal*, **1**, 193 (1955).
15. Quinton, J. H., and J. A. Storrow, *Chem. Eng. Sci.*, **5**, 245 (1956).
16. Singer, Emanuel, and R. H. Wilhelm, *Chem. Eng. Progr.*, **46**, 343 (1950).
17. Smith, J. M., "Chemical Engineering Kinetics," McGraw-Hill, New York (1956).
18. Strang, D. A., and C. J. Geankoplis, *Ind. Eng. Chem.*, **50**, 1305 (1958).
19. Wakao, Noriaki, Takashi Oshima, and Sakae Yagi, *Chem. Eng. (Japan)*, **22**, 780 (1958).
20. Wakao, Noriaki, and Sakae Yagi, *ibid.*, **23**, 161 (1959).
21. Wehner, J. F., and R. H. Wilhelm, *Chem. Eng. Sci.*, **6**, 89 (1956).
22. Yagi, Sakae, and Daizo Kunii, *A. I. Ch. E. Journal*, **3**, 373 (1957).

Manuscript received March 17, 1959; revision received December 31, 1959; paper accepted January 5, 1960.

APPENDIX

In the preceding sections the effective thermal conductivities were obtained with the assumption that there is no temperature difference between

the solid particle and the fluid. However it will be interesting to check the temperature difference. For this purpose the analysis with the simple model is carried out as shown below.

The heat conduction takes place both by means of the solid phase and the fluid phase. The steady state heat flow through the solid phase may be expressed with respect to the temperature of the solid as

$$\frac{K_s}{D_p^2}\frac{d^2t_s}{dZ^2} - h_p a(t_s - t_g) = 0 \quad (5)$$

The first term in Equation (5) represents the heat conduction in the solid-phase and the second term the heat transferred from solid to fluid. Heat transferred in the fluid phase is

$$\frac{C_pG}{D_p}\frac{dt_g}{dZ} + \frac{C_p\rho E}{D_p^2}\frac{d^2t_g}{dZ^2} + h_p a(t_s - t_g) = 0 \quad (6)$$

The first term in Equation (6) represents heat transport due to flow of air with the constant velocity and the second term the heat dispersed in the axial direction at a rate governed by the diffusivity. Hence the assumptions inherent in the above derivations are that t_s and t_g are functions of Z only; and K_s, $C_p\rho E$, and C_pG are everywhere constant in the bed, as far as the mean values are concerned.

The boundary conditions to be chosen are: 1. Radiation heat supplied to the solid section at the bed outlet face is equal to the enthalpy rise of fluid from the bed inlet to the outlet. 2. At a sufficiently deep region in the bed t_s and t_g approach the inlet fluid temperature; namely

$$Z = 0, \quad \frac{K_s}{D_p}\frac{dt_s}{dZ} + C_pG(t_{go} - t_i) = 0 \quad (7)$$

and

$$Z = \infty, t_s = t_g = t_i \quad (8)$$

Solutions to Equations (5) and (6) generally are expressed by the sum of the two negative exponential functions and one positive exponential function. By the boundary condition of Equation (8) the positive exponential function is excluded, and the solutions are formulated as follows:

$$\frac{t_g - t_i}{t_{go} - t_i} = \frac{1}{1 + b_o}(e^{-\lambda_1 Z} + b_o e^{-\lambda_2 Z}) \quad (9)$$

and

$$\frac{t_s - t_i}{t_{go} - t_i} = \frac{1}{1 + b_o}(b_1 e^{-\lambda_1 Z} + b_2 e^{-\lambda_2 Z}) \quad (10)$$

where λ_1 and λ_2 are the positive roots of

$$\lambda^3 - N_{Pe}\,\lambda^2 - N_{Nu}(a D_p)\left(\frac{N_{Pe}}{N_{Pr}N_{Re}} + \frac{k_g}{K_s}\right)\lambda + N_{Nu}N_{Pe}\,(a D_p)\frac{k_g}{K_s} = 0 \quad (11)$$

and b_0, b_1, and b_2 may be found by

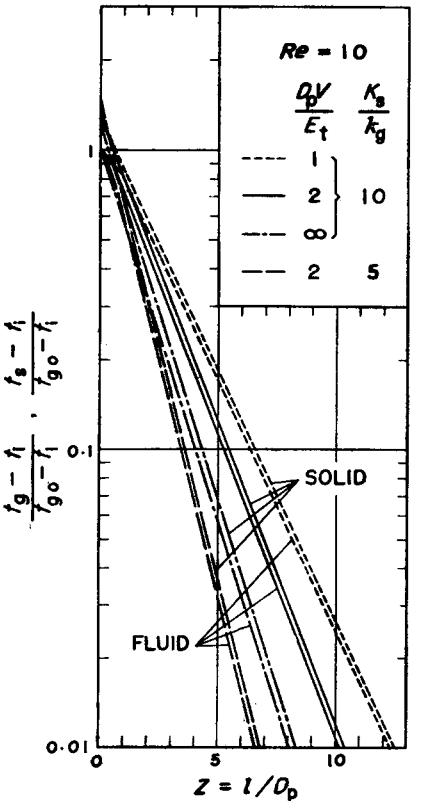

Fig. 5. Examples of calculated axial temperature gradients in solid and fluid phase.

$$b_1 = 1 + \frac{N_{Pr}N_{Re}}{N_{Nu}(a D_p)}\left\{\lambda_1 - \frac{\lambda_1^2}{N_{Pe}}\right\} \quad (12)$$

$$\frac{b_2}{b_o} = 1 + \frac{N_{Pr}N_{Re}}{N_{Nu}(a D_p)}\left\{\lambda_2 - \frac{\lambda_2^2}{N_{Pe}}\right\} \quad (13)$$

$$N_{Pr}N_{Re}\frac{k_g}{K_s} = \frac{b_1\lambda_1 + b_2\lambda_2}{1 + b_o} \quad (14)$$

For calculations of the above equations the values of E, h_p, and K_s are necessary. Axial effective diffusivity of fluid is the sum of the molecular thermal diffusivity and the turbulent eddy diffusivity of fluid E_t:

$$E = \epsilon\frac{k_g}{C_p\rho} + E_t \quad (15)$$

The correlation of the mass transfer coefficients (*19*) may be rewritten for the heat transfer coefficient as

$$N_{Nu} = \frac{h_p D_p}{k_g} = 2.0 + 1.45\,N_{Pr}^{1/3}N_{Re}^{1/2} \quad \text{for } N_{Re} < 100 \quad (16)$$

In addition to the above estimates and with the arbitrary assumption of the value of K_s being ten and five times as large as the molecular thermal conductivity of fluid k_g, the calculated results of Equations (9) and (10) are shown in Figure 5 in the case where $N_{Pr} = 0.70$ for air, $N_{Re} = 10$, and spherical packing and void fraction of bed $\epsilon = 0.4$. It is noted that the gradients of the axial temperatures are considerably affected by the extent of the fluid mixing and the value of K_s. In this illustration the value of K_s was arbitrarily assumed. On the other hand Singer and Wilhelm (*16*) have found that the thermal conductivity of the solid phase in radial direction of the bed was dependent upon the fluid velocity.

If the value of K_s is lower, the axial temperature gradients become steeper; however the difference between t_s and t_g is not considerable as far as the fluid velocity is relatively low. Therefore it will be permissible to neglect the temperature difference between solid and fluid and to introduce the concept of the axial effective thermal conductivity in the present investigations.

NOTATION

- a = specific surface area of solids in bed, 1/m.
- E = axial effective diffusivity of fluid including molecular-diffusion contribution, based on bed cross section, sq. m./hr.
- E_t = axial eddy diffusivity of fluid, based on bed cross section, sq. m./hr.
- h_p = heat transfer coefficient from solid to fluid, kcal./(sq. m)(hr.)(°C.)
- K_s = thermal conductivity of solid phase, based on bed cross section, kcal./(m.)(hr.)(°C.)
- N_{Nu} = h_pD_p/k_g = modified Nusselt number, dimensionless
- N_{Pe} = D_pV/E = modified Peclet number, dimensionless
- t_g = temperature of fluid, °C.
- t_{go} = temperature of effluent fluid, °C.
- t_s = temperature of solid, °C.
- V = superficial velocity of fluid, based on empty column, m./hr.
- Z = l/D_p = axial distance variable, dimensionless